

# Tuning the Nature of the Fluorescent State: A Substituted Polycondensed Dye as a Case Study

Cristina Sissa,<sup>[a]</sup> Valentina Calabrese,<sup>[b]</sup> Marco Cavazzini,<sup>[b]</sup> Luca Grisanti,<sup>[a]</sup>  
Francesca Terenziani,<sup>[a]</sup> Silvio Quici,<sup>[b]</sup> and Anna Painelli\*<sup>[a]</sup>

**Abstract:** An extensive spectroscopic analysis is presented of an elongated polycondensed dye with a donor–acceptor substitution. The charge-transfer (CT) state, polarized along the long molecular axis, is close in energy to a local excitation (LE) of the polycondensed system, roughly polarized along the short molecular axis, which makes this system particularly suitable to investigate the subtle LE/CT interplay. An essential-state model is presented

that quantitatively reproduces absorption and fluorescence spectra, as well as fluorescence emission and excitation anisotropy spectra collected in solvents of different polarity and viscosity, which sets a sound basis for the under-

standing of how solvent polarity and solvent relaxation affect the nature of low-lying excitations. The markedly different fluorescence emission and excitation anisotropy spectra measured in glassy and liquid polar solvents unambiguously demonstrate the major role played by solvent relaxation in the definition of fluorescence properties of the dye.

**Keywords:** donor–acceptor systems • dyes/pigments • essential-state models • fluorescence • solvatochromism

## Introduction

Basic understanding of spectroscopic signatures of charge-transfer (CT) states and processes dates back to the classical work of Robert Mulliken in 1952 on molecular complexes.<sup>[1]</sup> When two different molecules, D and A, come together in solution, a CT complex can be stabilized by the resonance between the neutral state, DA, and the zwitterionic state, D<sup>+</sup>A<sup>−</sup>, in which D labels the molecule that behaves as an electron donor with respect to the electron-accepting (A) molecule. A simple two-state model predicts not only the stabilization of the ground state due to resonance, but also the appearance of a low-lying excited state, responsible for the occurrence of a so-called CT transition in the visible or near-infrared spectral region, depending on the ionization potential of D, the electronic affinity of A, and the hopping integral between frontier molecular orbitals.<sup>[1–5]</sup>


The same Mulliken Hamiltonian has been successfully adopted to describe absorption spectra of mixed-valence systems,<sup>[6–12]</sup> and more recently to model optical spectra of

so-called push–pull chromophores,<sup>[13–21]</sup> an interesting class of elongated  $\pi$ -conjugated molecules bearing an electron-donor (D) and -acceptor (A) group at the two molecular ends. Intramolecular CT degrees of freedom in these  $\pi$ -conjugated systems share the same physics as intermolecular CT in molecular complexes, even if some differences are conveniently highlighted. In particular, in D- $\pi$ -A chromophores the two resonating states are coupled via virtual intermediate states in which charges are located in the bridge: the two-state model is therefore an effective model and, at variance with DA complexes, the D<sup>+</sup>- $\pi$ -A<sup>−</sup> dipole length cannot be estimated from the D-to-A physical distance.<sup>[9,22]</sup> The two-state model belongs to the more general class of essential-state models,<sup>[13–21,23–31]</sup> a family of parametric models developed to describe several families of CT chromophores. Essential-state models are parameterized and validated against experimental spectroscopic data, but recent attempts to extract relevant parameters from high-quality ab initio calculations appear very promising.<sup>[32–35]</sup>

The two-state model captures most of the physics of CT complexes but, already in the early days of the Mulliken model, the interaction between the CT state and other excited states, localized either on the D or the A molecule,<sup>[36,37]</sup> had been discussed to explain some anomalous spectral features. The distinction between CT and local excited (LE) states is clear-cut in molecular complexes, for which LE states can be mapped on the states of the two isolated neutral molecules, whereas the CT state describes the situation in which one electron is transferred from the D to the A molecule. The LE versus CT distinction is somewhat blurred in CT chromophores. However, based on a valence-bond description of the molecular electronic structure, the diabatic

[a] Dr. C. Sissa, Dr. L. Grisanti, Prof. F. Terenziani, Prof. A. Painelli  
Dipartimento di Chimica  
Università di Parma and INSTM UdR-Parma  
Parco Area delle Scienze 17A, 43124 Parma (Italy)  
Fax: (+39) 0521-905556  
E-mail: anna.painelli@unipr.it

[b] Dr. V. Calabrese, Dr. M. Cavazzini, Dr. S. Quici  
Istituto di Scienze e Tecnologie Molecolari (ISTM)  
Consiglio Nazionale delle Ricerche (CNR)  
via C. Golgi 19, 20133 Milano (Italy)

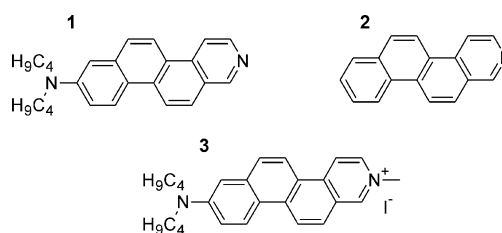
 Supporting information for this article is available on the WWW under <http://dx.doi.org/10.1002/chem.201202154>.

CT state corresponding to  $D^+-\pi-A^-$  is easily defined as the state having the maximum charge separation or the maximum dipole moment along the D–A direction.<sup>[38]</sup> The definition of CT transitions is extremely useful in spectroscopy. CT transitions involve electronic states with a large contribution from the  $D^+-\pi-A^-$  state, and are characterized by a large variation of the molecular dipole moment upon excitation. Experimentally, absorption and fluorescence bands associated with CT transitions show a strong solvatochromism and a considerable inhomogeneous broadening in polar solvents.<sup>[39]</sup>

The interplay between CT and LE states in CT chromophores shows up in the most spectacular way with dual-fluorescence phenomena.<sup>[40–46]</sup> Strictly speaking, dual fluorescence applies to systems, like *N,N*-dimethylaminobenzonitrile (DMABN), that show in the same solvent two distinct fluorescence bands. In these systems a detectable fluorescence signal is observed not only from the lowest singlet state, according to the Kasha rule,<sup>[47]</sup> but also from a higher-energy state. Breaking the Kasha rule is of course possible, provided that the lifetime of the higher-energy fluorescent state is long enough: double fluorescence then not only requires CT/LE competition driven by polar solvation, but also the coupling to some slow (conformational) degree of freedom, to slow down the conversion between the two forms and give time for the system to fluoresce from both states.<sup>[40–46]</sup> In a more relaxed definition, double fluorescence describes systems for which the fluorescence can be obtained from different states according to experimental conditions.<sup>[48]</sup> For LE/CT systems, in particular, the fluorescent state can switch from LE to CT upon increasing the solvent polarity.<sup>[48–50]</sup> In this case, a single fluorescence band is observed in each solvent, the Kasha rule is fulfilled, and there are no special requirements about the relative lifetime of excited states.

The possibility to switch the fluorescent state from a LE to a CT state is of interest for all applications, such as natural or artificial light-harvesting systems, for which charge separation is sought after photoexcitation.<sup>[51–53]</sup> At the same time, environment-dependent fluorescence is of interest for applications in sensing and biosensing.<sup>[54–57]</sup> The broad emission from CT states can be usefully exploited for organic light-emitting devices: the charge separation, which influences the intersystem-crossing yield, can strongly affect the overall device efficiency.<sup>[58]</sup> Recognizing the nature of the fluorescent state is, however, a nontrivial task: a strong solvent dependence of fluorescence spectra, in terms of frequency and band shapes, is in fact expected for several families of organic chromophores with a pure CT character, even in the absence of LE/CT competition.<sup>[23, 59–65]</sup>

Herein, we present a detailed study of a 2-azachrysene substituted in position 8 by a dibutylamino group (**1** in Scheme 1). This dye is related to an interesting family of polycondensed dyes extensively studied by Fromherz and co-workers for voltage-sensing applications in biologically relevant environments.<sup>[66–68]</sup> The dibutylamino group acts as a good electron donor (D) with respect to the aza-substituted

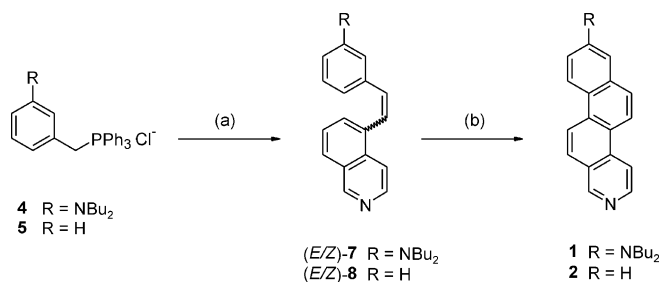


Scheme 1. Molecular structures of the investigated dyes.

ed benzene ring, which in turn acts as an acceptor (A). A low-lying CT excitation is therefore expected for this dye, polarized along the D–A axis, roughly coincident with the long molecular axis. According to the Platt description of electronic excitation in polyacenes,<sup>[69]</sup> the lowest electronic excitation of chrysene is assigned to a  $^1L_b$  state, polarized along the short molecular axis, and with a very weak intensity.<sup>[70]</sup> A localized state with  $^1L_b$  character is therefore also expected in aza-substituted chrysene and related molecules, even if its precise position is difficult to guess. In any case, for the molecules discussed in this study a low-lying LE state is expected, roughly polarized along the short molecular axis and hence making a sizable angle with the direction of polarization of the CT absorption. Under these conditions, fluorescence anisotropy spectra offer detailed information on the nature of excited states. Based on recent advances in the theoretical simulation of anisotropy spectra in polar solvents,<sup>[71]</sup> a detailed study of the spectral properties of **1** and related dyes offers a clear-cut demonstration of the evolution of the nature of the fluorescent state from LE in nonpolar solvents to CT in polar solvents.

## Results

**Materials:** The materials used in the present study were prepared in good yields by careful modification of a known literature procedure.<sup>[67]</sup> The compound 8-(*N,N*-dibutylamino)-2-azachrysene **1** (Scheme 2) was obtained through a modified procedure previously reported<sup>[72]</sup> by some of us, which consists in a Wittig condensation of (3-*N,N*-dibutylamino)-benzyltriphenylphosphonium chloride **4** with isoquinoline-5-carbaldehyde **6**, followed by a photochemical cyclization of



Scheme 2. a) Isoquinoline-5-carbaldehyde **6**, *t*BuOK, dry THF,  $N_2$ , reflux, overnight; b)  $CH_2Cl_2$ ,  $h\nu$ , 16 h, 15 °C.

the mixture of diastereoisomeric alkenes (*E*)- and (*Z*)-**7** so obtained. The corresponding methylated salt **3** was simply prepared by reaction of compound **1** with MeI in THF.<sup>[72]</sup> Similarly, the unsubstituted 2-azachrysene **2** was synthesized by photochemical cyclization of a mixture of (*E*)- and (*Z*)-5-aminostyrylisoquinoline **8** that was obtained by Wittig reaction between benzyltriphenylphosphonium chloride (**5**) and isoquinoline-5-carbaldehyde (**6**).

**Optical properties:** The solvents used for spectroscopic studies are listed in Table 1. We selected a set of solvents with similar refractive index and increasing dielectric constant, to

Table 1. Properties of solvents used for spectroscopic studies.

Solvent	Dielectric constant	Refractive index	Kamlet–Taft $\alpha$ parameter
cyclohexane (CH)	2.0	1.43	0.00 <sup>[73]</sup>
toluene (Tol)	2.4	1.50	0.00 <sup>[73]</sup>
2-MeTHF	7.0	1.41	0.00 <sup>[73],[a]</sup>
CH <sub>2</sub> Cl <sub>2</sub>	8.9	1.42	0.13 <sup>[73]</sup>
propylene glycol (PrGly)	32.1	1.43	0.83 <sup>[74]</sup>
DMSO	46.7	1.48	0.00 <sup>[73]</sup>

[a] The parameter refers to tetrahydrofuran.

span a wide range of solvent polarity. To avoid specific interactions, namely H-bonding interactions involving the aza group in **1** and **2**,<sup>[75]</sup> solvents were selected with poor H-donating characteristics (see the Kamlet–Taft  $\alpha$  parameter in Table 1). Indeed propylene glycol (PrGly), the only solvent with a mild H-donating character, was considered because it is one of the few polar solvents that can be frozen in glassy matrices, as needed for fluorescence anisotropy spectra. In any case, as discussed below, all spectra measured at ambient conditions in PrGly practically coincide with those measured in DMSO, thus confirming that, with reference to the molecules of interest in this study, PrGly behaves as a polar solvent with a similar polarity to that of DMSO. In PrGly a secondary emission appears at  $\approx 620$  nm that, according to lifetime data (see the Supporting Information), is safely ascribed to an excimer emission and will not be further discussed.

Absorption and fluorescence spectra of the dibutylamino-substituted azachrysene dye (**1**) dissolved in solvents of different polarity are reported in Figure 1. The most interesting feature of the absorption spectrum is the intense band located at 350–370 nm: this band, which shows a pronounced solvatochromism and an important broadening in polar solvents, can be safely ascribed to a CT absorption polarized along the D–A axis (roughly parallel to the long molecular axis). At lower energy, two weak absorption features are clearly seen in cyclohexane and in mildly polar solvents (up to 2-methyltetrahydrofuran (2-MeTHF)). In more polar solvents, the CT band moves to the red and overlaps these small features.

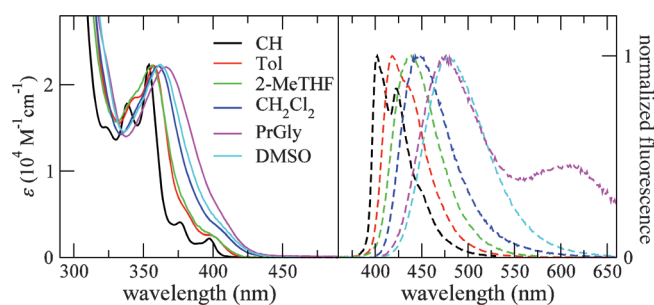


Figure 1. Absorption (left panel, full lines) and emission spectra (right panel, dashed lines) of **1** in solvents of different polarity. The molar extinction coefficient  $\epsilon$  axis refers to CH<sub>2</sub>Cl<sub>2</sub> solutions; absorption spectra in other solvents are normalized to the same maximum.

To understand the physical origin of these weak features, we collected absorption and fluorescence spectra of the unsubstituted azachrysene dye **2**. The absorption spectra of **2** (top panel of Figure 2) show an intense absorption at  $\approx 300$  nm (not shown here; see the Supporting Information in which other spectra of **2**, including fluorescence, are reported), which can be ascribed to allowed transitions of the polycondensed rings polarized along the long molecular axis. More relevant to our discussion is the weak absorption feature ( $\epsilon \approx 3000 \text{ M}^{-1} \text{ cm}^{-1}$  in CH<sub>2</sub>Cl<sub>2</sub> and DMSO) with a well-resolved vibronic structure centered around 350 nm. This weak absorption can be assigned to a nominally forbidden transition (<sup>1</sup>L<sub>b</sub> in the Platt scheme for unsubstituted polyacenes) polarized along the short molecular axis.<sup>[69,70]</sup> The transition does not imply any important variation of the molecular dipole moment; accordingly, the absorption band is nonsolvatochromic and does not broaden in polar solvents.

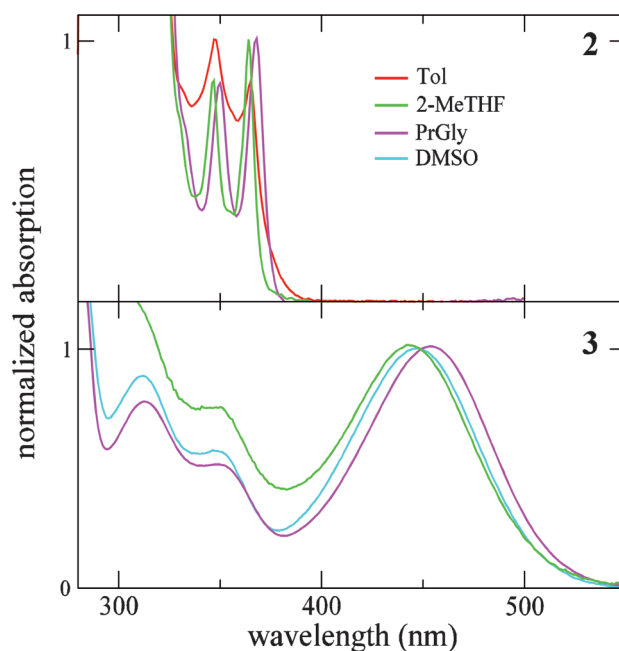


Figure 2. Absorption spectra of **2** (top panel) and **3** (bottom panel) in different solvents.

We therefore tentatively assign the small features observed to the red of the main (CT) absorption band of **1** to a localized (vibrationally resolved) transition, polarized along the short molecular axis.

For comparison, the bottom panel of Figure 2 shows the absorption spectra of dye **3**, a derivative of **1** with a methylated aza group. This group is a much stronger electron acceptor than the non-methylated group; accordingly, the absorption band related to the CT transition is redshifted with respect to **2**, falling in a spectral region well separated from the LE transition. The low-energy spectral features observed for **3** are therefore safely described as a pure CT transition.

Fluorescence spectra of **1** (Figure 1) show the typical solvatochromism of CT states, with an important redshift in polar solvents and an increasing Stokes shift with solvent polarity. The band-shape evolution also resembles what is often observed for polar dyes,<sup>[59–63]</sup> with a well-resolved vibronic structure in cyclohexane and a progressive increase of inhomogeneous broadening with increasing solvent polarity. Based on the similarity with the behavior of polar dyes, it is tempting to assign the fluorescence band to the CT transition. However, in cyclohexane the 0–0 emission band is exactly superimposed on the weak lowest-energy absorption band, assigned to the LE (0–0 vibronic) transition. Moreover, according to the Kasha rule,<sup>[47]</sup> one expects fluorescence from the lowest-energy singlet state. On this basis, the fluorescence signal measured in cyclohexane can be assigned to the LE transition. However, the character of the fluorescence band apparently changes to CT in more polar solvents, as demonstrated by its pronounced solvatochromism, by the large Stokes shifts, and by the conspicuous inhomogeneous broadening, strongly suggesting a double-fluorescence behavior for **1**.

Partial support of this hypothesis is obtained from a detailed analysis of fluorescence lifetimes. Table 2 collects the fluorescence quantum yields,  $\Phi$ , and fluorescence lifetimes,  $\tau_f$ , measured for the three compounds in solvents of different polarity. From these data we can estimate the radiative lifetime,  $\tau_0 = \tau_f / \Phi$  (i.e., the inverse emission radiative rate). Being unaffected by the rate of nonradiative processes, similar  $\tau_0$  values are expected for similar processes occurring in different media. According to the data in Table 2,  $\tau_0$  is marginally solvent dependent for **2**. The corresponding value is very similar to that estimated for **1** in cyclohexane, thus sup-

porting the description of the relevant excitation as due to a LE state. With increasing solvent polarity, the radiative lifetime of **1** decreases fast, reaching a value of  $\approx 20$  ns in DMSO, as expected for a CT state. Indeed the strong CT character of the low-lying transition of dye **3** leads to an even shorter  $\tau_0$  ( $\approx 10$  ns).

The different direction of polarization of the LE (roughly parallel to the short molecular axis) and CT transition (roughly parallel to the long molecular axis) in **1** suggests that further experimental support of the intriguing hypothesis of an evolution of the fluorescence band from LE to CT with solvent polarity can be gained through detailed measurements of fluorescence anisotropy spectra. Emission and excitation anisotropy spectra collected for **1–3** in glassy matrices obtained upon fast cooling of 2-MeTHF and PrGly solutions are shown in Figure 3.

A thorough understanding of the complex behavior of anisotropy spectra of **1** requires a detailed model of the LE/CT interplay and is deferred to the next section. Here we

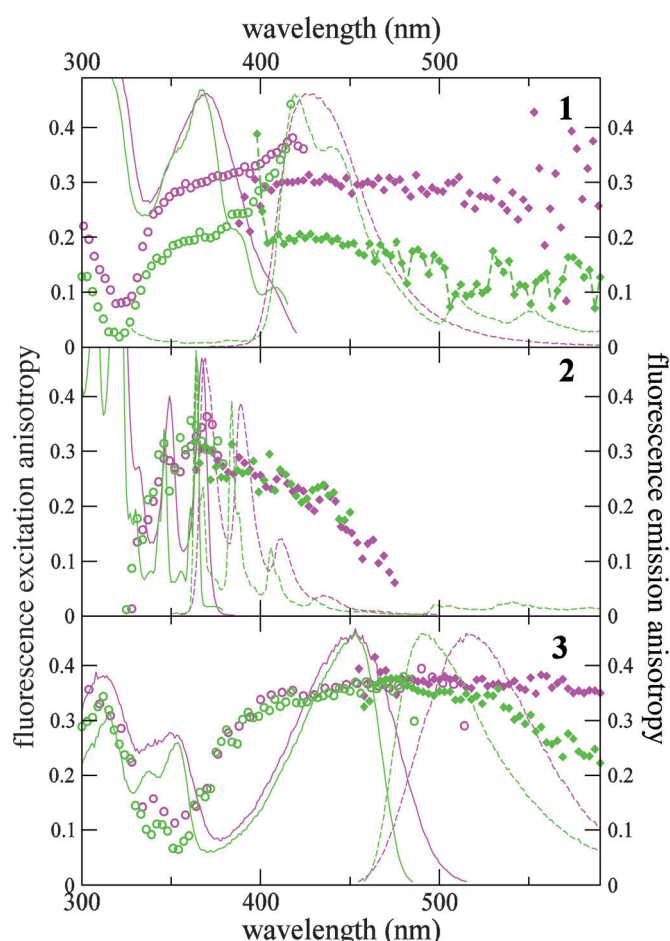


Figure 3. Fluorescence excitation (circles) and emission (diamonds) anisotropy spectra in glassy 2-MeTHF at 77 K (green) and PrGly at 200 K (violet), and the corresponding fluorescence excitation (full lines) and emission (dashed lines) spectra of compounds **1–3**. For **1** and **3**, fluorescence emission/excitation spectra were collected exciting/detecting at the maximum of absorption/emission; for **2**, due to the superposition of the vibronic 0–0 lines in absorption and emission, spectra were excited/detected at the maximum of the 0–1 line.

Table 2. Wavenumber at maximum fluorescence intensity ( $\bar{\nu}_f$ ), fluorescence quantum yields ( $\Phi$ ), fluorescence lifetimes ( $\tau_f$ ), and radiative lifetimes ( $\tau_0$ ).

Molecule	Solvent	$\bar{\nu}_f$ [cm <sup>-1</sup> ]	$\Phi$	$\tau_f$ [ns]	$\tau_0$ [ns]
<b>1</b>	CH	24 900	0.22	7.6	34.5
	Tol	24 000	0.25	6.7	26.8
	CH <sub>2</sub> Cl <sub>2</sub>	22 600	0.25	5.1	20.4
	DMSO	21 100	0.52	9.9	19.0
<b>2</b>	Tol	27 300	0.20	7.9	39.5
	CH <sub>2</sub> Cl <sub>2</sub>	27 300	0.18	6.7	37.2
	DMSO	27 100	0.33	10.3	31.2
<b>3</b>	CH <sub>2</sub> Cl <sub>2</sub>	16 200	0.61	5.5	9.0
	DMSO	15 600	0.36	3.6	10.0



observe that fluorescence spectra collected in glassy polar solvents are qualitatively different from those collected in the same *liquid* solutions. In the liquid phase, after the solute photoexcitation the surrounding molecules of the polar solvent reorient themselves in response to the variation of the charge distribution in the solute, which favors the emission from a CT state. This reorientation is not possible in glassy matrices so that, irrespective of solvent polarity, emission occurs from a LE state. Indeed, fluorescence spectra measured in glassy polar solvents (2-MeTHF and PrGly, Figure 3) closely resemble spectra measured in nonpolar or mildly polar liquid solvents (see Figure 1). In line with this interpretation, the fluorescence excitation anisotropy is close to the limiting value,  $r=0.4$ , on the red edge of the absorption band, that is, in the region of the LE absorption, and decreases fast in the region of the CT absorption. Although this interpretation sounds appealing and is correct to a first approximation, the detailed modeling in the next section suggests a somewhat more complex picture.

Anisotropy spectra of **2**, with  $r \approx 0.4$  in the region of the vibronic 0–0 transition, confirm that the emission signal comes from the same state involved in the absorption process. The progressive decrease of  $r$  on moving away from the 0–0 line suggests that the vibrational modes responsible for the vibronic progression are polarized along a different direction with respect to the electronic transition. Spectra of **3** are easily interpreted: in the region of the main absorption and fluorescence bands, both emission and excitation anisotropy are close to the limiting  $r=0.4$  value, which confirms that absorption and fluorescence involve the same state, with dominant CT character.

**Modeling the LE/CT interplay:** Optical spectra of polar D- $\pi$ -A chromophores (in which  $\pi$  is a conjugated bridge) can be quantitatively described based on a two-state model that is an extension of the Mulliken model,<sup>[1,2]</sup> also accounting for molecular vibrations and polar solvation.<sup>[59–65]</sup> As in the Mulliken model, the electronic Hamiltonian is written on the basis of two diabatic states corresponding to the limiting valence-bond structures, D- $\pi$ -A and D<sup>+</sup>- $\pi$ -A<sup>−</sup>. The two states are separated by an energy  $2\eta$ , and mixed by a matrix element  $\langle \text{D-}\pi\text{-A} | H | \text{D}^+\text{-}\pi\text{-A}^- \rangle = -\tau$ . The dipole moment associated with D<sup>+</sup>- $\pi$ -A<sup>−</sup>,  $\mu_0$ , is very large, and all other matrix elements of the dipole-moment operator on the chosen basis are neglected. An effective vibrational coordinate,  $Q$ , is introduced to describe the vibronic structure of optical spectra: the two basis states are assigned two harmonic potential energy surfaces with the same frequency,  $\omega_v$ , but displaced minima, to introduce a linear dependence on  $Q$  of the energy gap between the two basis states:  $2\eta - \sqrt{2}\varepsilon_v\omega_v Q$ , in which  $\varepsilon_v$  is the vibrational relaxation energy associated with the charge-separated basis state. Polar solvation is described by introducing the polar component of the reaction field  $F$ , that is, the electric field that is generated at the solute location due to the reorientation of polar solvent molecules around the polar solute. If the solute is described as a continuum elastic medium,  $F$  enters

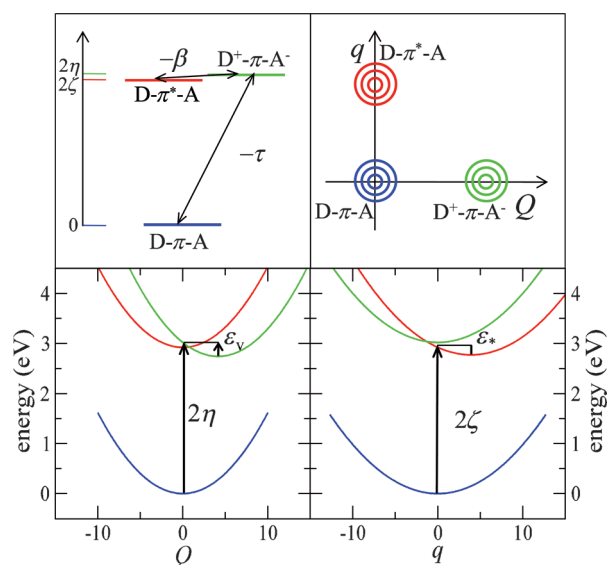


Figure 4. Sketch of the proposed model. The top-left panel defines the energies of the three electronic basis states and the corresponding mixing matrix elements ( $-\tau$  and  $-\beta$ ). The top-right panel shows the contour plots for the diabatic potential energy surfaces associated with the three electronic states in the  $Q, q$  plane. The two bottom panels show cuts of the same potential energy surfaces along the  $q=0$  (left) and  $Q=0$  (right) planes.

the problem as a classical coordinate, and polar solvation is fully described by  $\varepsilon_{or}$ , the solvent reorganization energy (associated with the D<sup>+</sup>- $\pi$ -A<sup>−</sup> basis state).

This very simple model proved successful for the calculation of linear (absorption and fluorescence) and nonlinear (two-photon absorption, second- and third-harmonic generation, etc.) spectra of several push-pull chromophores,<sup>[59–65]</sup> and is therefore expected to capture the basic physics of the CT transition in **1**. However, it cannot describe the LE state. To model the complex interplay between the LE and CT states, we therefore extend the standard model to introduce a third state, D- $\pi^*$ -A, which describes the LE state related to the low-energy excitation observed in the substituted azachrysene dye. We assign this state an energy  $2\zeta$  and, according to early suggestions,<sup>[49,76]</sup> we account for the coupling between this state and D<sup>+</sup>- $\pi$ -A<sup>−</sup>:  $\langle \text{D-}\pi^*\text{-A} | H | \text{D}^+\text{-}\pi\text{-A}^- \rangle = -\beta$ . We neglect the direct coupling between the LE state D- $\pi^*$ -A and the neutral D- $\pi$ -A state, in view of the high energy difference between the two states. We assume that the D- $\pi^*$ -A state is displaced with respect to D- $\pi$ -A along an effective vibrational coordinate,  $q$ , with frequency  $\omega_*$  and relaxation energy  $\varepsilon_*$ . A sketch of the relevant model is given in Figure 4.

The total Hamiltonian reads [Eq. (1)]:

$$H = \begin{pmatrix} 0 & -\tau & 0 \\ -\tau & 2\eta - \omega_v \sqrt{2}\varepsilon_v Q - F & -\beta \\ 0 & -\beta & 2\zeta - \omega_* \sqrt{2}\varepsilon_* q \end{pmatrix} + \frac{P^2 + \omega_v^2 Q^2}{2} + \frac{p^2 + \omega_*^2 q^2}{2} + \frac{F^2}{4\mu_0^2 \varepsilon_{or}} \quad (1)$$

in which  $P$  and  $p$  are the conjugated momenta of  $Q$  and  $q$ , respectively.

According to Mulliken,<sup>[1,2]</sup> in the two-state model the dipole-moment operator is defined just in terms of  $\mu_0$ , the dipole moment of the zwitterionic  $D^+-\pi-A^-$  state, which is very large if compared with the other matrix elements of the dipole-moment operator, so that one can safely approximate  $\langle D-\pi-A | \mu | D-\pi-A \rangle = \langle D^+-\pi-A^- | \mu | D-\pi-A \rangle = 0$ . We stick to this approximation but, to account for the small intensity of the LE transition, we introduce an additional matrix element of the dipole-moment operator:  $\langle D-\pi-A | \mu | D-\pi^*-A \rangle = \mu_*$ . This dipole moment makes an angle  $\varphi$  with the  $D-A$  axis, parallel to  $\mu_0$ . Fixing the  $x$  direction along  $\mu_0$ , the two matrices representing the  $x$  and  $y$  components of the dipole-moment operator then read [Eqs. (2) and (3)]:

$$\mu_x = \begin{pmatrix} 0 & 0 & \mu_* \cos \varphi \\ 0 & \mu_0 & 0 \\ \mu_* \cos \varphi & 0 & 0 \end{pmatrix} \quad (2)$$

$$\mu_y = \begin{pmatrix} 0 & 0 & \mu_* \sin \varphi \\ 0 & 0 & 0 \\ \mu_* \sin \varphi & 0 & 0 \end{pmatrix} \quad (3)$$

Strictly speaking, the total dipole-moment operator, defined by the two matrices in Equations (2) and (3), should be used in the effective Hamiltonian to describe polar solvation. Accordingly, two components of the reaction field ( $F_x$  and  $F_y$ ) should be introduced as independent variables, thus leading to a numerically intensive calculation. However, on a physical basis, we expect  $\mu_* \ll \mu_0$ , so that solvation effects related to  $\mu_*$  are negligible. Estimated model parameters fully confirm this working hypothesis, with  $\mu_0 > 20\mu_*$  (see Table 3).

The Hamiltonian in Equation (1) describes three electronic states coupled to two vibrational modes and to a solvation coordinate. The solvation coordinate is related to a very slow motion and is treated in the adiabatic approximation. Specifically, the Hamiltonian is defined on a grid of  $F$  values. For each  $F$  value, the Hamiltonian describing the coupled electron-vibration problem is written on the basis obtained as the direct product of the three electronic basis states and the eigenstates of the two harmonic oscillators associated with  $Q$  and  $q$ . The nominally infinite bases associated with the two oscillators are truncated to the first  $M$

lowest states, to make the problem numerically tractable. The Hamiltonian matrix (dimension  $3M^2$ ) is diagonalized to get nonadiabatic eigenstates that represent a numerically exact solution provided  $M$  is large enough to guarantee convergence ( $M=8-10$  was used in this work). Transition energies and transition and permanent dipole moments are then easily evaluated, as needed for the calculation of optical spectra, according to the equations reported as Supporting Information. Optical spectra calculated for each point of the  $F$ -grid are finally mediated over all  $F$  values, thereby weighting each spectrum for the relevant Boltzmann distribution (see the Supporting Information for more details).

## Discussion

Figure 5 shows absorption and fluorescence spectra calculated for **1** with optimized model parameters (reported in Table 3) and with increasing  $\epsilon_{or}$  values (reported in Table 4)

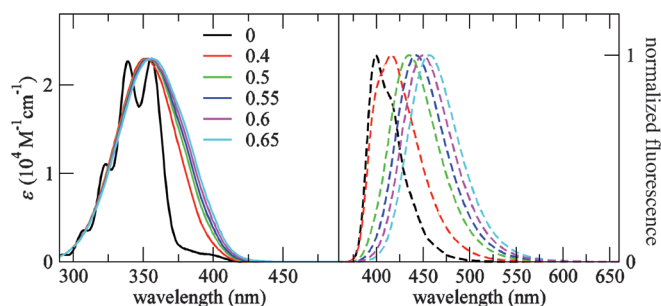


Figure 5. Calculated absorption and emission spectra of **1** according to parameters reported in Table 3 and for different  $\epsilon_{or}$  values [eV] corresponding to solvents of different polarity. The extinction coefficient axis refers to  $\epsilon_{or}=0.55$  eV, as relevant to  $CH_2Cl_2$ ; other spectra are normalized to the same maximum.

Table 4. Solvent parameters entering the calculation of the optical spectra of **1**.

Solvent	$\epsilon_{or}$ [eV]	Solvent	$\epsilon_{or}$ [eV]
CH	0.00	PrGly	0.60
Tol	0.40	DMSO	0.65
2-MeTHF	0.50	glycerol	0.75
$CH_2Cl_2$	0.55		

to mimic increasing solvent polarity. The LE feature is clearly seen in the low-energy wing of the calculated absorption spectrum at  $\epsilon_{or}=0$ . The progressive redshift and broadening of the CT band with increasing  $\epsilon_{or}$  nicely reproduces the evolution of experimental spectra with increasing solvent polarity. Emission frequencies and band shapes and their evolution with solvent polarity are similarly well reproduced.

Table 3. Molecular model parameters entering the calculation of the optical spectra of **1**, as discussed in the text.  $\Gamma=0.075$  eV is the effective intrinsic width assigned to each transition (see the Supporting Information).

$\eta$ [eV]	$\tau$ [eV]	$\zeta$ [eV]	$\beta$ [eV]	$\mu_0$ [D]	$\mu_*$ [D]	$\varphi$ [°]	$\epsilon_v$ [eV]	$\omega_v$ [eV]	$\epsilon_*$ [eV]	$\omega_*$ [eV]
1.51	1.07	1.46	0.04	19.6	0.85	50	0.28	0.18	0.15	0.14

To understand the concept of dual fluorescence and to shed light on the optical spectra of **1**, Figure 6 shows the energies of the ground and fluorescent states calculated as a function of  $F$ . The color of the curve relevant to the fluorescent state gives information about its nature: the red versus

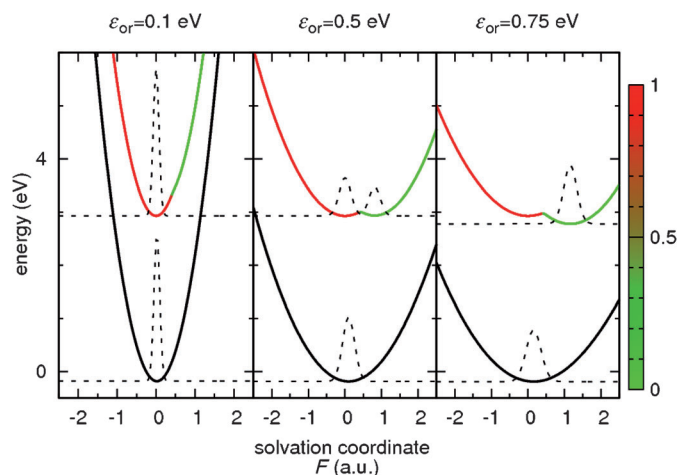


Figure 6. Full lines: the energy of the ground and fluorescent states calculated as functions of the reaction field  $F$  for the model parameters reported in Table 3 and three  $\epsilon_{\text{or}}$  values. The color scale on the right refers to the curve relevant to the fluorescent state and measures the weight of the CT state (pure red corresponds to pure LE character, pure green to pure CT character). Dashed lines: probability distributions of the reaction field  $P_{\text{gs}}(F)$  and  $P_{\text{fluo}}(F)$  calculated at 300 K.

green proportions are related to the weight of the LE state versus the weight of the CT state (the CT state is a mixture of D- $\pi$ -A and D<sup>+</sup>- $\pi$ -A<sup>-</sup>, so its weight is simply obtained as the complement to 1 of the weight of the LE state). The change in color, and hence in the nature of the lowest excited state, is fairly abrupt, in line with the small value of  $\beta$ , the matrix element that mixes LE and CT states (see Table 3), which suggests that the direct mixing between the two states can be safely neglected except in a narrow region of  $F$  values in which the two diabatic CT and LE states are almost degenerate.

Figure 6 also reports the Boltzmann distributions associated with the ground and fluorescent states:  $P_{\text{gs}}(F) \propto \exp[-E_{\text{gs}}(F)/(kT)]$  and  $P_{\text{fluo}}(F) \propto \exp[-E_{\text{fluo}}(F)/(kT)]$ , in which  $E_{\text{gs}}$  and  $E_{\text{fluo}}$  are the energies of the ground and excited states, respectively,  $k$  is the Boltzmann constant, and  $T$  the absolute temperature. The ground-state distribution,  $P_{\text{gs}}$ , enters the calculation of absorption spectra as well as of fluorescence spectra in glassy matrices, whereas the fluorescent-state distribution,  $P_{\text{fluo}}$ , is relevant to the calculation of (steady-state) fluorescence spectra in liquid solutions.

The “regular” form of the ground-state energy curve implies a typical bell-shaped ground-state distribution, the width of which increases with solvent polarity, thus supporting increasing inhomogeneous spectral broadening in polar solvents. More interesting is the behavior of the fluorescent state: for all  $\epsilon_{\text{or}}$  values, the nature of the *vertical* excitation is

essentially pure LE, but upon increasing  $F$  it changes abruptly to CT (corresponding curves in Figure 6 change color abruptly from red to green). For medium to large  $\epsilon_{\text{or}}$  values (middle and right panels, Figure 6), the fluorescent-state energy shows two minima along the reaction field coordinate, one with LE character and the other with CT character. For intermediate  $\epsilon_{\text{or}}$  values the two minima are within thermal energy and one observes a bimodal probability distribution. Turning to the spectra, for low  $\epsilon_{\text{or}}$  values the potential energy surfaces in the left panels of Figure 6 show that the lowest-energy absorption, which occurs on the vertical, has a pure LE character and hence a small transition dipole moment (related to  $\mu_{\text{e}}$ ). In agreement with experimental data, a second much more intense vertical absorption is expected towards a higher-energy state (its potential energy curve is not shown in Figure 6) with a pure CT character. The relaxed excited state responsible for steady-state fluorescence has again a pure LE character. At intermediate  $\epsilon_{\text{or}}$  values (middle panel, Figure 6), the vertical excitation leads again mainly to a state with pure LE character. However, due to the finite width of the ground-state distribution, states with at least a partial CT nature give a small yet sizable contribution to the absorption spectrum. In view of the high intensity associated with the CT process if compared with the LE transition, the marginal contribution of CT transitions actually dominates the observed (and calculated) absorption spectrum in solvents of intermediate polarity. Emission comes from the equilibrated fluorescent state that, for  $\epsilon_{\text{or}}=0.5$ , has a comparable population of both the LE and CT states. In other terms, due to thermal disorder, fluorescence in intermediate-polarity solutions arises with similar proportions from the LE state of molecules experiencing a small reaction field and from the CT state of molecules experiencing a sizable reaction field. This is not clearly evident from experimental (and calculated) spectra that are again largely dominated by the CT emission, in view of its large transition dipole moment.

In strongly polar solvents ( $\epsilon_{\text{or}}=0.75$ , right panel in Figure 6) the vertical absorption is again mainly driving the system towards a LE state, yet the spectrum is largely dominated by the (marginal) contribution from the CT transition, mainly because of its comparatively large transition dipole moment. The relaxed fluorescent state, however, is now a pure CT state, with a negligible thermal population of the LE state: emission in this case has an essentially pure CT character.

This complex theoretical picture leads to an impressive agreement with experimental spectra in Figure 1, a nontrivial achievement, strongly supporting the reliability of the proposed model. An even more stringent validation of the model and of relevant parameters can be obtained from the analysis of fluorescence anisotropy spectra. According to a recently devised computational strategy,<sup>[71]</sup> briefly summarized in the Supporting Information, we are in a position to calculate fluorescence excitation and emission anisotropy spectra, fully accounting for polar solvation. The spectra in Figure 7 have been calculated for **1** by adopting exactly the

same model used for the spectra in Figure 5 and fixing the temperature (entering the Boltzmann distribution, see the Supporting Information) to the glass transition temperature of 2-MeTHF (90 K) and PrGly (200 K).

In glassy matrices, the solvent molecules cannot change their orientation in response to the photoexcitation of the solute, so that the distribution of the reaction field stays fixed at the distribution relevant to the solute in the ground state. Therefore, as sketched in Figure 8, in the calculation

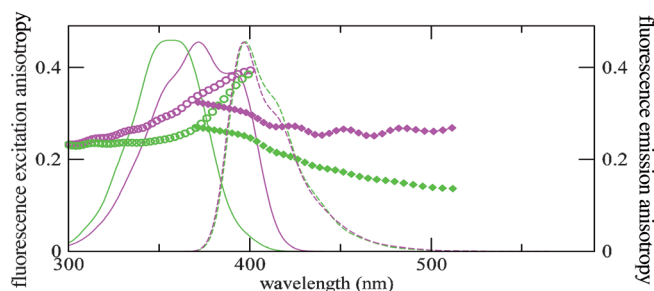


Figure 7. Calculated fluorescence excitation anisotropy (circles) and fluorescence emission anisotropy (diamonds) of **1** in 2-MeTHF (green) at 90 K and PrGly (violet) at 200 K, and the corresponding fluorescence excitation (full lines) and emission (dashed lines) spectra. Fluorescence emission/excitation spectra are calculated by fixing the excitation/detection wavelengths at 357/400 nm.

of fluorescence emission and excitation spectra and of the relevant anisotropies in glassy matrices, the same distribution of the reaction field must be adopted as introduced in the calculation of absorption spectra (of course at the relevant temperature). As a result, irrespective of the solvent polarity, in glassy solvents fluorescence mainly comes from the LE state: in line with experimental data, the calculated fluorescence in glassy solvents is nonsolvatochromic. Moreover, fluorescence excitation anisotropy is high ( $r \approx 0.4$ ) in the red edge of the fluorescence excitation profile, dominated by the LE absorption, and decreases at higher energies, at which the excitation acquires a CT nature.

The main differences between the spectra in 2-MeTHF and PrGly are related to the different glass transition temperatures. 2-MeTHF vitrifies at 90 K, so that the corresponding reaction-field distribution is much narrower than for PrGly, with a glass transition temperature of 200 K. At 200 K a sizable population is calculated of states with a mixed LE/CT character, which leads to a smoother switching from LE to CT than in 2-MeTHF, as supported by the slope of the fluorescence excitation anisotropy. Although the calculated anisotropy spectra in 2-MeTHF compare very well with experimental data, the fluorescence excitation spectrum calculated in PrGly is somewhat redshifted. This is most probably related to an overestimated intensity from the mixed CT/LE region. Indeed, better results would be obtained by fixing the temperature to 90 K also in this solvent. A temperature difference of 110 K corresponds to  $\approx 0.01$  eV, a fairly acceptable energy mismatch within the scope of the present model.

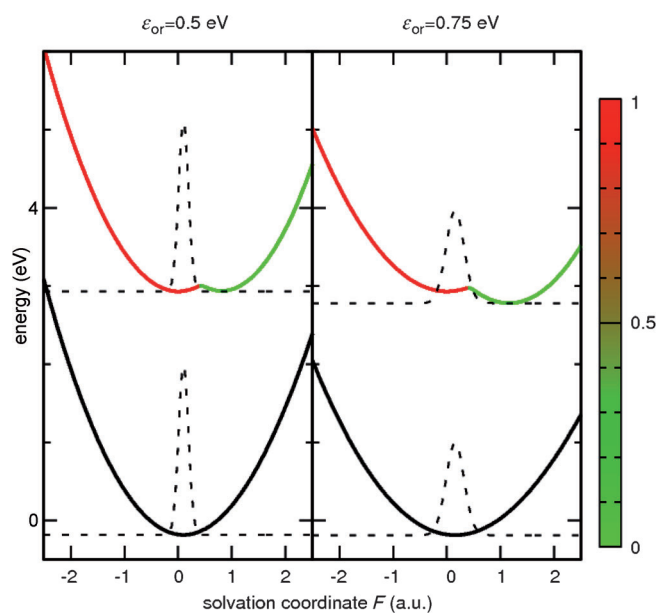


Figure 8. Full lines: energy of the ground and fluorescent states calculated as functions of the reaction field  $F$  for the model parameters reported in Table 3 and two  $\epsilon_{or}$  values. The color scale on the right refers to the curve relevant to the fluorescent state and measures the weight of the CT state (pure red corresponds to pure LE character, pure green to pure CT character). Dashed lines: probability distributions of the reaction field relevant to the ground state  $P_{gs}(F)$  (as needed for the calculation of optical spectra in glassy matrices) calculated at 90 K for  $\epsilon_{or}=0.5$ , as relevant to 2-MeTHF glassy matrices (left panel), and at 200 K for  $\epsilon_{or}=0.75$ , as relevant to undercooled glycerol (right panel).

In glassy solvents fluorescence spectra are largely dominated by the LE transition, mainly because under these conditions the large reaction fields needed to stabilize the CT state have negligibly small probabilities. It is therefore interesting to study fluorescence anisotropy spectra in polar non-glassy solvents, to gain information about fluorescence from the CT state. Reliable fluorescence anisotropy data can be obtained only in liquid solvents viscous enough to hinder the solute reorientation in the timescale of the excited-state lifetime, thus making the solute reorientation a slower process than fluorescence. As discussed in references [26] and [77], glycerol satisfies these requirements. The top panels of Figure 9 show the fluorescence excitation and relevant anisotropy spectra of **1** in liquid glycerol (room temperature, left panel) and in an undercooled glycerol matrix (200 K, right panel). As expected, due to the similar polarity of the two solvents, spectra collected in glassy glycerol resemble closely those collected in glassy PrGly (see Figure 3). More interesting are spectra collected in liquid glycerol (room temperature). In liquid polar solvents the CT state is stabilized by the solvent relaxation, so that, as seen in the right panel of Figure 6, fluorescence arises from a pure CT state. Indeed, the observed anisotropy is fairly large ( $r > 0.3$ ) and basically flat in the region of the CT absorption, showing just a small dip in the red wing of the excitation band, at which the LE transition contributes to the excitation spectrum. The corresponding calculated spectra, reported in the



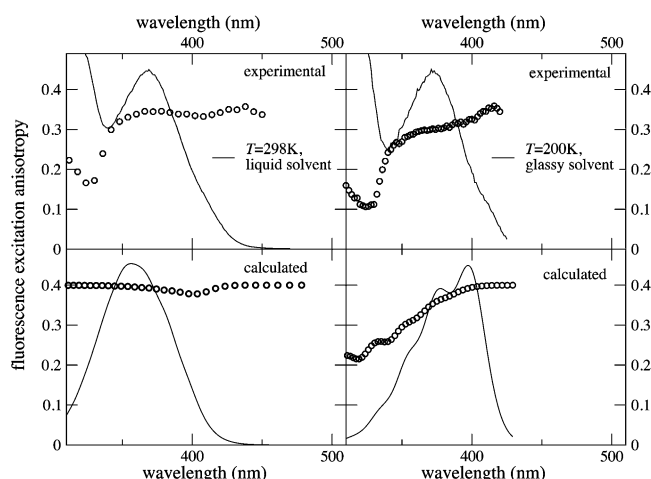


Figure 9. Experimental (top panels) and calculated (bottom panels) fluorescence excitation spectra (full lines) and fluorescence excitation anisotropy spectra (circles) of **1** in glycerol at room temperature (liquid phase, left panels) and at 200 K (glassy phase, right panels). Fluorescence excitation anisotropy spectra were collected by detecting the fluorescence signal at the maximum of the emission spectra. The model parameter  $\epsilon_{\text{or}}$  relevant to the solvent relaxation is set to 0.75 eV for glycerol. Fluorescence emission spectra are reported in the Supporting Information.

bottom panels of Figure 9, quantitatively reproduce the experimental spectra, hence offering very strong support of the proposed picture.

## Conclusion

The concept of CT states and excitations was introduced 60 years ago with reference to molecular complexes formed in solution by the encounter between an electron donor (D) and an acceptor (A) molecule.<sup>[1,2]</sup> The absorption spectra of the complex show bands that have no counterpart in solutions of either the isolated D or A molecules. These bands, assigned to CT processes, are usually located to the red of local excitations characteristic of either the D or A molecules: their comparatively low energy is related to the low ionization potential of D, the high electron affinity of A, and the (usually very small) intermolecular hopping integral. CT bands of molecular complexes are very broad and structureless: thermal disorder in the relative orientation and distance between the two molecules forming the complex modulates the intermolecular hopping integral, thus representing a very effective source of inhomogeneous spectral broadening. The sum rule for the oscillator strength imposes that the intensity associated with the CT absorption is borrowed from LE states. However, the success of the Mulliken model<sup>[1,2]</sup> demonstrates that, in most cases, the LE–CT interactions need not be explicitly accounted for.

Concepts and models developed to describe intermolecular CT processes in molecular complexes proved extremely useful to set up the basis of current understanding of intramolecular CT in  $\pi$ -conjugated D- $\pi$ -A (or push–pull) chromophores. Although sharing many similarities, the two fami-

lies of systems are distinctively different. The first obvious difference is that when dealing with intramolecular CT, that is, with systems in which the D and A groups are bound together in a single molecular structure, there are no spectra of the isolated D and A species for comparison: singling out spectral features due to the CT excitation is then more delicate than for CT complexes. Most often and fairly reliably, CT excitations are recognized based on their distinctive dependence on solvent polarity. CT transitions in fact induce large variations of the molecular dipole moment leading to an important solvatochromism that was recognized early.<sup>[39,78,79]</sup>

At variance with intermolecular CT, intramolecular CT occurs in well-defined molecular structures and, apart from a few cases in which electrons are strongly coupled to low-frequency conformational degrees of freedom,<sup>[80,81]</sup> electronic energies are modulated by high-frequency vibrations that appear in optical spectra with well-defined vibronic progressions rather than with inhomogeneous broadening phenomena. Polar solvation is a specific source of inhomogeneous broadening in push–pull chromophores;<sup>[21,59–65,82]</sup> thermal disorder in the orientation of polar solvent molecules is in fact responsible for a distribution of solvent reaction fields at the solute location, with inhomogeneous broadening effects that increase fast with the solvent polarity. In nonpolar solvents, however, there are no effective mechanisms for inhomogeneous broadening of intramolecular CT transitions, and many examples are known of CT absorption (and fluorescence) bands with a well-resolved vibronic structure.<sup>[59–65]</sup>

The possibility of controlling the nature of the excited state, switching it from a LE state (typically a  $\pi$ – $\pi^*$  excitation marginally affected by solvent polarity) to a CT state with its distinctive solvatochromism, opens an interesting scenario with important applicative implications,<sup>[51–58]</sup> which offers an intriguing challenge to theoreticians and spectroscopists. Dual fluorescence, with the concomitant appearance of two fluorescence bands in the same spectrum, gives a clear indication of LE/CT interplay, even if the detailed interpretation of the phenomenon is somewhat controversial.<sup>[40–46]</sup> Dual fluorescence is a rare phenomenon that requires a very precise balance between the fluorescence lifetimes of the two involved states and their interconversion velocity, to guarantee the observation of sizable steady-state fluorescence from both states.

Although not so striking as dual fluorescence, the observation of the evolution of fluorescence spectra from a LE emission to a CT emission upon increasing solvent polarity is a clear signature of LE/CT interplay. Double fluorescence in this more relaxed definition is a rare phenomenon as well: though somewhat independent of excited-state lifetimes, it requires a LE state lower in energy than the CT state in nonpolar solvents, but not too far from the CT state, so that polar solvents can stabilize the CT state below the LE state. The delicate issue is how to assign, in these systems, the emission to the CT or the LE transition. The evolution of spectral band shapes with the solvent polarity is not a guarantee for LE-to-CT evolution: in fact, at variance

with the common paradigm, established in the field of CT complexes, narrow CT bands with a well-resolved vibronic structure are routinely observed for push–pull chromophores in nonpolar solvents.<sup>[59–65]</sup>

Herein, we have presented an extensive analysis of a push–pull dye based on a polycondensed ring (azachrysene) structure, which exhibits a delicate balance between a low-lying LE state of the polyaromatic system and the CT state. Clear signatures of the LE state are recognized in absorption spectra in which, at least in nonpolar or weakly polar solvents, a weak and vibronically resolved band is observed just to the red of the more intense CT transition. Upon increasing solvent polarity, the CT band redshifts and broadens overlapping the small LE features. In the nonpolar solvent (cyclohexane) the fluorescence band is characterized by a negligible Stokes shift and is therefore safely ascribed to a LE transition. The important fluorescence solvatochromism definitely suggests that in polar solvents the fluorescent state acquires a CT nature.

The resulting picture is fairly complex and efforts to build reliable models must rely on an extensive set of experimental data. The noncollinear polarization of the CT and LE transitions in this system makes fluorescence anisotropy spectra extremely informative. Anisotropy spectra collected in two glassy matrices obtained from solvents of different polarity as well as in a liquid viscous solvent quite unambiguously point to the important role of the reorientation of the polar solvent molecules after the solute photoexcitation as the driving mechanism stabilizing the CT state.

The extensive set of spectroscopic data collected on dye **1** allowed us to define and validate a reliable model fully accounting for the complex interplay between LE and CT states. The proposed model shares the same basic physics with early models for the LE/CT competition (or somewhat analogous spectral phenomena) based on three electronic states.<sup>[13–19,76]</sup> Herein, the model is extended to account for the coupling of electronic degrees of freedom with molecular vibrations and with an effective polar solvation coordinate. Moreover, by exploiting numerical techniques recently developed in the framework of essential-state models,<sup>[23,59–65,71]</sup> for the first time we are able to quantitatively reproduce the complete spectral evolution of the system with solvent polarity. With a minimal set of optimized model parameters we calculate absorption, fluorescence, and fluorescence anisotropy spectra of the chromophore, as well as their solvent dependence, and reproduce not only the spectral position but also—which is much more challenging—the relevant band shapes. The proposed model is general, and indeed we explicitly verified its applicability to an analogue of chromophore **1** with three rather than four condensed rings (a substituted azaphenanthrene). Relevant results are reported in the Supporting Information.

An important and nontrivial issue emerging from the analysis concerns the role of thermal disorder associated with polar solvation. The LE/CT interplay implies that, at least in some solvents, the energy gap between the two excited states is comparable to the thermal energy, so that

both states are thermally populated. Under these conditions the observed fluorescence is actually a superposition of the signals due to the CT and the LE emission, actually leading to a dual fluorescence in the strict definition. The two signals, however, occur in the same spectral region so that the two contributions show an important spectral overlap.

In conclusion, a thorough experimental and theoretical analysis proves unambiguously that the nature of the fluorescent state of dye **1** evolves from a pure LE state in nonpolar solvents to a pure CT state in strongly polar solvents. Solvent relaxation after photoexcitation plays a major role in the stabilization of the CT state, so that in glassy matrices emission mainly comes from the LE state, irrespective of the solvent polarity. Thermal population of both states is expected in solvents of intermediate polarity, which leads to the simultaneous emission from both states, even if relevant spectral effects are difficult to single out due to the spectral overlap of the two signals.

## Experimental Section

**General:** All commercially available solvents and reagents were used as received without further purification. 8-(*N,N*-Dibutylamino)-2-azachrysene (**1**) and the corresponding methylated salt (**3**) were prepared according to the procedure previously reported by us. For a detailed description of their synthesis and characterization, see ref. [72]. Thin-layer chromatography (TLC) was conducted on plates precoated with silica gel Si 60-F254 (Merck, Darmstadt, Germany). Column chromatography was carried out on silica gel Si 60, mesh size 0.040–0.063 mm (Merck, Darmstadt, Germany). <sup>1</sup>H and <sup>13</sup>C NMR spectra were recorded on a Bruker Avance 400 spectrometer (400 and 100.6 MHz, respectively). Chemical shifts are indicated in parts per million downfield from SiMe<sub>4</sub>, with the residual proton (CHCl<sub>3</sub>,  $\delta$  = 7.26 ppm) and carbon (CDCl<sub>3</sub>,  $\delta$  = 77.0 ppm) solvent resonances as internal reference. ESI mass spectra were recorded on a Thermo Finnigan LCQ Advantage spectrometer equipped with an electrospray ion trap and an electrospray ion-trap mass spectrometer ICR-FTMS APEX II (Bruker Daltonics) by the Centro Interdipartimentale Grandi Apparecchiature (C.I.G.A.) of the University of Milano.

**Benzyltriphenylphosphonium chloride (5):** PPh<sub>3</sub> (2.48 g, 9.4 mmol) was added to a solution of benzyl chloride (1.00 g, 7.9 mmol) in heptane (10 mL) and the mixture was heated at reflux for 24 h. After cooling to room temperature, the white precipitate was isolated by filtration and washed with heptane and Et<sub>2</sub>O, then dried in vacuo to afford pure **5** (2.73 g, 7.03 mmol, 89%). <sup>1</sup>H NMR (400 MHz, CDCl<sub>3</sub>):  $\delta$  = 7.78–7.73 (m, 9H; Ar-*H*), 7.63–7.27 (m, 6H; Ar-*H*), 7.20 (m, 1H; Ar-*H*), 7.10 (m, 4H; Ar-*H*), 5.53 ppm (d, <sup>1</sup>*J*(H,P) = 15 Hz, 2H; CH<sub>2</sub>P); <sup>13</sup>C NMR (100.6 MHz, CDCl<sub>3</sub>):  $\delta$  = 134.86 (*J*(C,P) = 2.3 Hz; CH), 134.42 (*J*(C,P) = 9.8 Hz; CH), 131.60 (*J*(C,P) = 5.4 Hz; CH), 130.10 (*J*(C,P) = 12.4 Hz; CH), 128.78 (*J*(C,P) = 2.7 Hz; CH), 128.28 (*J*(C,P) = 3.7 Hz; CH), 127.43 (*J*(C,P) = 8.9 Hz; C), 118.06 (*J*(C,P) = 85.4 Hz; C), 30.67 ppm (*J*(C,P) = 46.3 Hz; CH<sub>2</sub>); HRMS (ESI): *m/z*: calcd for C<sub>25</sub>H<sub>22</sub>P<sup>+</sup>: 353.15 [*M*–Cl]<sup>+</sup>; found: 353.2; elemental analysis calcd (%) for C<sub>25</sub>H<sub>22</sub>PCl: C 77.22, H 5.70; found: C 77.19, H 5.71.

**(*E,Z*)-5-Styrylisoquinoline (8):** Benzyltriphenylphosphonium chloride **5** (2.00 g, 5.14 mmol) was dissolved in dry THF (40 mL) under a nitrogen atmosphere, *t*BuOK (656 mg, 5.37 mmol) was added, and the solution was heated at reflux. Isoquinoline-5-carbaldehyde **6** (735 mg, 4.68 mmol) dissolved in dry THF (5 mL) was then added and the reaction mixture was heated at reflux overnight. The solvent was concentrated in vacuo, then a solution of hexane/AcOEt (4:1 v/v, 20 mL) was added to promote the precipitation of triphenylphosphine oxide. The solid formed was isolated by filtration, and the solution was evaporated in vacuo. The crude product was purified by column chromatography (silica gel, 1:1 hexane/

AcOEt) to afford **8** (615 mg, 2.66 mmol, 51.7%) as a mixture of diastereoisomers. Minimum amounts of pure (*E*)-5-styrylisoquinoline and (*Z*)-5-styrylisoquinoline were isolated only for NMR characterization. (*Z*)-**8**: <sup>1</sup>H NMR (400 MHz, CDCl<sub>3</sub>): δ = 9.27 (s, 1H), 8.50 (d, <sup>3</sup>J(H,H) = 5.4 Hz, 1H), 7.89 (d, <sup>3</sup>J(H,H) = 8.1 Hz, 1H), 7.81 (d, <sup>3</sup>J(H,H) = 5.4 Hz, 1H), 7.58 (d, <sup>3</sup>J(H,H) = 7.1 Hz, 1H), 7.48 (t, <sup>3</sup>J(H,H) = 8.1 Hz, 1H), 7.07–7.12 (m, 3H), 7.02–7.05 (m, 2H), 6.96 (d, <sup>3</sup>J(H,H) = 12 Hz, 1H), 6.89 ppm (d, <sup>3</sup>J(H,H) = 12 Hz, 1H); <sup>13</sup>C NMR (100.6 MHz, CDCl<sub>3</sub>): δ = 153.95, 143.22, 136.44, 136.30, 134.40, 134.18, 133.30, 130.67, 128.96, 128.20, 127.44, 127.05, 126.99, 126.46, 117.83 ppm. (*E*)-**8**: <sup>1</sup>H NMR (400 MHz, CDCl<sub>3</sub>): δ = 9.27 (s, 1H), 8.58 (d, <sup>3</sup>J(H,H) = 6 Hz, 1H), 7.91–8.00 (m, 3H), 7.78 (d, <sup>3</sup>J(H,H) = 16 Hz, 1H), 7.60–7.65 (m, 3H), 7.42 (t, <sup>3</sup>J(H,H) = 7.3 Hz, 2H), 7.31–7.35 (m, 2H), 7.22 ppm (d, <sup>3</sup>J(H,H) = 16 Hz, 1H); <sup>13</sup>C NMR (100.6 MHz, CDCl<sub>3</sub>): δ = 153.19, 143.32, 137.12, 134.08, 133.96, 132.80, 128.86, 128.23, 127.38, 127.25, 127.11, 126.80, 123.84, 116.67 ppm; HRMS (ESI): *m/z*: calcd for C<sub>17</sub>H<sub>14</sub>N<sup>+</sup>: 232.1126 [*M*+H]<sup>+</sup>; found: 232.1120; elemental analysis calcd (%) for C<sub>17</sub>H<sub>13</sub>N: C 88.28, H 5.67, N 6.06; found: C 88.38, H 5.65, N 6.08.

**2-Azachrysene (2):** A magnetically stirred solution of (*E*)- and (*Z*)-5-styrylisoquinoline **8** (518 mg, 2.24 mmol) in CH<sub>2</sub>Cl<sub>2</sub> (500 mL) was irradiated by a Hg high-pressure lamp in a quartz reactor for 16 h at 15 °C. The mixture was concentrated to a small volume, which allowed the precipitation of 2-azachrysene (**2**) that was collected by filtration. After evaporation to dryness of the remaining solution, the solid residue was rinsed with Et<sub>2</sub>O, thus affording a second crop of compound **2** (410 mg, total yield 80%). <sup>1</sup>H NMR (400 MHz, CDCl<sub>3</sub>): δ = 9.36 (s, 1H), 8.78–8.84 (m, 3H), 8.64 (d, <sup>3</sup>J(H,H) = 8.8 Hz, 1H), 8.49 (d, <sup>3</sup>J(H,H) = 6 Hz, 1H), 8.02–8.10 (m, 3H), 7.69–7.78 ppm (m, 2H); <sup>13</sup>C NMR (100.6 MHz, CDCl<sub>3</sub>): δ = 152.20, 144.78, 134.55, 133.09, 130.64, 130.21, 128.78, 128.16, 127.39, 127.14, 126.61, 125.58, 123.47, 122.74, 120.79, 116.35 ppm; HRMS (ESI): *m/z*: calcd for C<sub>17</sub>H<sub>12</sub>N<sup>+</sup>: 230.0970 [*M*+H]<sup>+</sup>; found: 230.0962; elemental analysis calcd (%) for C<sub>17</sub>H<sub>11</sub>N: C 89.06, H 4.84, N 6.11; found: C 89.20, H 4.85, N 6.09.

**Spectroscopic measurements:** Solvents used for spectroscopic measurements: cyclohexane (CH), Sigma–Aldrich, Chromasolv plus ≥ 99.9%; toluene (Tol), Sigma–Aldrich, Chromasolv plus ≥ 99.9%; 2-methyltetrahydrofuran (2-MeTHF), anhydrous ≥ 99%; dichloromethane (CH<sub>2</sub>Cl<sub>2</sub>), Sigma–Aldrich, Chromasolv plus ≥ 99.9%; propylene glycol (PrGly), Riedel-de Haën, 99.5%; dimethyl sulfoxide (DMSO), Riedel-de Haën, 99.5%; glycerol, Sigma–Aldrich, anhydrous ≥ 99.5%. All solvents were used as received, except 2-MeTHF, which was stored overnight over molecular sieves (0.3 nm).

Absorption spectra were collected on a Perkin–Elmer Lambda 650 spectrometer on solutions of concentration ≈ 10<sup>−5</sup> M, which verified the Beer–Lambert law for measurements of the molar extinction coefficient. Fluorescence emission and excitation spectra were measured on a Horiba JobinYvon Fluoromax-3 spectrofluorometer equipped with a xenon arc lamp as light source, on dilute solutions (≈ 10<sup>−6</sup> M) to minimize self-absorption. Fluorescein in NaOH 0.1 M (fluorescence quantum yield = 0.9) was used as the standard for the determination of the fluorescence quantum yields. Fluorescence decays were recorded with the same spectrofluorometer, in time-correlated single-photon counting (TCSPC) mode, by using different nano-LEDs as pulsed excitation sources. The same instrument, equipped with emission and excitation Glan–Thompson automatic polarizers, was used to measure fluorescence anisotropy, defined as [Eq. (4)]:

$$r = \frac{I_{\parallel} - I_{\perp}}{I_{\parallel} + 2I_{\perp}} \quad (4)$$

in which *I*<sub>∥</sub> is the fluorescence intensity when emission and excitation polarizers are parallel, and *I*<sub>⊥</sub> is the fluorescence intensity when the two polarizers are orthogonal.<sup>[47]</sup> Fluorescence anisotropy spectra were measured in viscous media or in rigid matrices, to avoid depolarization caused by rotational diffusion. Glycerol at room temperature is viscous enough to avoid diffusion,<sup>[26,77]</sup> whereas other measurements were performed in glassy 2-MeTHF (after rapid cooling at 77 K) and undercooled PrGly

(after rapid cooling at 200 K). Further information on fluorescence anisotropy measurements can be found in ref. [71].

## Acknowledgements

This work was partially supported by the Fondazione Cariparma through the Project 2010.0329 and by the Italian Ministry of University and Research (MIUR) through the Project FIRB-Futuro in Ricerca RBFR10Y5VW. C.S. thanks the University of Parma and INSTM for financial support.

- [1] R. S. Mulliken, *J. Am. Chem. Soc.* **1952**, *74*, 811–824.
- [2] R. S. Mulliken, W. B. Person, *Molecular Complexes*, Wiley, New York, **1969**.
- [3] Z. G. Soos, D. J. Klein, in *Molecular Associations, Vol. 1*, (Ed. R. Foster), Academic Press, New York, **1971**, p. 1.
- [4] A. Painelli, A. Girlando, *J. Chem. Phys.* **1987**, *87*, 1705–1711.
- [5] C. Pecile, A. Painelli, A. Girlando, *Mol. Cryst. Liq. Cryst.* **1989**, *171*, 69–87.
- [6] N. S. Hush, *Prog. Inorg. Chem.* **1967**, *8*, 391–444.
- [7] N. S. Hush, *Coord. Chem. Rev.* **1985**, *64*, 135–157.
- [8] N. S. Hush, J. R. Reimers, *Chem. Rev.* **2000**, *100*, 775–786.
- [9] M. Bixon, J. Jortner, *Adv. Chem. Phys.* **1999**, *106*, 35–202.
- [10] J. Jortner, J. Ulstrup, *J. Chem. Phys.* **1973**, *63*, 4358–4368.
- [11] J. Jortner, M. J. Bixon, *J. Chem. Phys.* **1988**, *88*, 167–170.
- [12] J. Cortes, H. Heitele, J. Jortner, *J. Phys. Chem.* **1994**, *98*, 2527–2536.
- [13] D. R. Kanis, M. A. Ratner, T. Marks, *J. Chem. Res.* **1994**, *94*, 195–242.
- [14] S. R. Marder, B. Kippelen, A. K.-Y. Jen, N. Peyghambarian, *Nature* **1997**, *388*, 845–851.
- [15] J. Brédas, K. Cornil, F. B. D. Meyers, In *Handbook of Conducting Polymers*, 2nd ed. (Eds: T. A. Skotheim, R. L. Elsenbaumer, J. R. Reynolds), Marcel Dekker, New York, **1998**, p. 1.
- [16] J. L. Oudar, D. S. Chemla, *J. Chem. Phys.* **1977**, *66*, 2664–2668.
- [17] S. R. Marder, D. N. Beratan, L.-T. Cheng, *Science* **1991**, *252*, 103–106.
- [18] G. Chen, J. W. Perry, W. A. Goddard, *J. Am. Chem. Soc.* **1994**, *116*, 10679–10685.
- [19] W. H. Thompson, M. Blanchard-Desce, V. Alain, J. Muller, A. Fort, M. Barzoukas, J. T. Hynes, *J. Phys. Chem. A* **1999**, *103*, 3766–3771.
- [20] A. Painelli, *Chem. Phys. Lett.* **1998**, *285*, 352–359.
- [21] A. Painelli, *Chem. Phys.* **1999**, *245*, 185–197.
- [22] L. Grisanti, G. D’Avino, A. Painelli, J. Guash, I. Ratera, J. Veciana, *J. Phys. Chem. B* **2009**, *113*, 4718–4725.
- [23] F. Terenziani, A. Painelli, C. Katan, M. Charlot, M. Blanchard-Desce, *J. Am. Chem. Soc.* **2006**, *128*, 15742–15755.
- [24] F. Terenziani, O. V. Przhonska, S. Webster, L. A. Padilha, Y. L. Slominsky, I. G. Davydenko, A. O. Gerasov, Y. P. Kovtun, M. P. Shandura, A. D. Kachkovski, *J. Phys. Chem. Lett.* **2010**, *1*, 1800–1804.
- [25] C. Sissa, F. Terenziani, A. Painelli, A. Abboto, L. Bellotto, C. Marini, E. Garbin, C. Ferrante, R. Bozio, *J. Phys. Chem. B* **2010**, *114*, 882–893.
- [26] C. Sissa, F. Terenziani, A. Painelli, R. B. Kanth Siram, S. Patil, *J. Phys. Chem. B* **2012**, *116*, 4959–4966.
- [27] C. Sissa, P. Mohamadzadeh Jahani, Z. G. Soos, A. Painelli, *ChemPhysChem* **2012**, *13*, 2795–2800.
- [28] F. Terenziani, C. Sissa, A. Painelli, *J. Phys. Chem. B* **2008**, *112*, 5079–5087.
- [29] C. Sissa, V. Parthasarathy, D. Drouin-Kucma, M. H. V. Verts, M. Blanchard-Desce, F. Terenziani, *Phys. Chem. Chem. Phys.* **2010**, *12*, 11715–11727.
- [30] J. Campo, A. Painelli, F. Terenziani, T. Van Regemorter, D. Beljonne, E. Goovaerts, W. Wenseleers, *J. Am. Chem. Soc.* **2010**, *132*, 16467–16478.
- [31] F. Terenziani, G. D’Avino, A. Painelli, *ChemPhysChem* **2007**, *8*, 2433–2444.

- [32] S. Olsen, R. H. McKenzie, *J. Chem. Phys.* **2009**, *130*, 184302–184314.
- [33] S. Olsen, *J. Chem. Theory Comput.* **2010**, *6*, 1089–1103.
- [34] S. Olsen, R. H. McKenzie, *J. Chem. Phys.* **2011**, *134*, 114520–114532.
- [35] S. Olsen, *J. Phys. Chem. A* **2012**, *116*, 1486–1492.
- [36] J. N. Murrell, *J. Chem. Phys.* **1959**, *81*, 5037–5043.
- [37] S. Masaki, T. M. N. Okada, Y. Sakat, S. Misumi, *Bull. Chem. Soc. Jpn.* **1976**, *49*, 1277–1283.
- [38] T. Van Voorhis, T. Kowalczyk, B. Kaduk, L.-P. Wang, C.-L. Cheng, Q. Wu, *Annu. Rev. Phys. Chem.* **2010**, *61*, 149–170.
- [39] C. Reichardt, *Chem. Rev.* **1994**, *94*, 2319–2358.
- [40] Z. R. Grabowski, K. Rotkiewicz, W. Rubaszewska, E. Kirrór-Kaminska, *Acta Physica Polonica* **1978**, *A54*, 767–776.
- [41] K. A. Zachariasse, *Chem. Phys. Lett.* **2000**, *320*, 8–13.
- [42] W. Rettig, S. Lutze, *Chem. Phys. Lett.* **2001**, *341*, 263–271.
- [43] A. B. J. Parusel, W. Retting, K. Rotkiewicz, *J. Phys. Chem. A* **2002**, *106*, 2293–2299.
- [44] Z. R. Grabowski, K. Rotkiewicz, W. Retting, *Chem. Rev.* **2003**, *103*, 3899–4031.
- [45] T. Yoshihara, S. I. Druzhinin, K. A. Zachariasse, *J. Am. Chem. Soc.* **2004**, *126*, 8535–8539.
- [46] A. Demeter, S. I. Druzhinin, A. A. Kovalenko, T. A. Senyushkina, K. A. Zachariasse, *J. Phys. Chem. A* **2011**, *115*, 1521–1537.
- [47] J. R. Lakowicz, *Principles of Fluorescence Spectroscopy*, Kluwer Academic/Plenum Publishers, New York, **1999**.
- [48] F. B. Dias, S. Pollock, G. Hedley, L.-O. Pålsson, A. P. Monkman, I. Perepichka, I. F. Perepichka, M. Tavalis, M. R. Bryce, *J. Phys. Chem. B* **2006**, *110*, 19329–19339.
- [49] J. Herbich, A. Kapturkiewicz, *J. Am. Chem. Soc.* **1998**, *120*, 1014–1029.
- [50] N. Banerji, G. Angulo, I. Barabanov, E. Vauthey, *J. Am. Chem. Soc.* **2008**, *130*, 9665–9674.
- [51] S. Günes, H. Neugebauer, N. Sariciftci, *Chem. Rev.* **2007**, *107*, 1324–1338.
- [52] M. Grätzel, *Acc. Chem. Res.* **2009**, *42*, 1788–1798.
- [53] J. Roncali, *Acc. Chem. Res.* **2010**, *43*, 1716–1730.
- [54] M. S. T. Gonçalves, *Chem. Rev.* **2009**, *109*, 190–212.
- [55] M. Y. Berezin, S. Achilefu, *Chem. Rev.* **2010**, *110*, 2641–2684.
- [56] H. Kobayashi, M. Hogawa, R. Alford, P. U. Y. Choike, *Chem. Rev.* **2010**, *110*, 2620–2640.
- [57] G. Signore, R. Nifosi, L. Albertazzi, B. Storti, R. Bizzarri, *J. Am. Chem. Soc.* **2010**, *132*, 1276–1288.
- [58] S. M. King, R. Matheson, F. B. Dias, A. P. Monkman, *J. Phys. Chem. B* **2008**, *112*, 8010–8016.
- [59] B. Boldrini, E. Cavalli, A. Painelli, F. Terenziani, *J. Phys. Chem. A* **2002**, *106*, 6286–6294.
- [60] F. Terenziani, A. Painelli, A. Girlando, R. M. Metzger, *J. Phys. Chem. B* **2004**, *108*, 10743–10750.
- [61] A. Painelli, F. Terenziani, L. Angiolini, T. Benelli, L. Giorgini, *Chem. Eur. J.* **2005**, *11*, 6053–6063.
- [62] L. Grisanti, C. Sissa, F. Terenziani, A. Painelli, D. Roberto, F. Tesore, R. Ugo, S. Quici, I. Fortunati, E. Garbin, *Phys. Chem. Chem. Phys.* **2009**, *11*, 9450–9457.
- [63] F. Todescato, I. Fortunati, S. Carlotto, C. Ferrante, L. Grisanti, C. Sissa, A. Painelli, A. Colombo, C. Dragonetti, D. Roberto, *Phys. Chem. Chem. Phys.* **2011**, *13*, 11099–11109.
- [64] L. Grisanti, F. Terenziani, C. Sissa, M. Cavazzini, F. Rizzo, S. Orlandi, A. Painelli, *J. Phys. Chem. B* **2011**, *115*, 11420–11430.
- [65] C. Sissa, F. Terenziani, A. Painelli, A. K. Manna, S. K. Pati, *Chem. Phys.* **2012**, *404*, 9–15.
- [66] C. Röcker, A. Heilemann, P. Fromherz, *J. Phys. Chem.* **1996**, *100*, 12172–12177.
- [67] G. Hübener, A. Lambacher, P. Fromherz, *J. Phys. Chem. B* **2003**, *107*, 7896–7902.
- [68] B. Kuhn, P. Fromherz, *J. Phys. Chem. B* **2003**, *107*, 7903–7913.
- [69] J. R. Platt, *J. Chem. Phys.* **1949**, *17*, 484–495.
- [70] P. N. Skancke, *Acta Chem. Scand.* **1965**, *19*, 401–413; H. B. Kleven, J. R. Platt, *J. Chem. Phys.* **1949**, *17*, 470–481; N. A. Borisevich, G. G. Dyachenko, V. A. Petukhov, M. A. Semenov, *Optics and Spectroscopy* **2008**, *105*, 859–866.
- [71] C. Sissa, A. Painelli, M. Blanchard-Desce, F. Terenziani, *J. Phys. Chem. B* **2011**, *115*, 7009–7020.
- [72] S. Quici, V. Calabrese, E. Rossi, E. Cariati, C. Dragonetti, D. Roberto, E. Tordin, F. De Angelis, S. Fantacci, *Chem. Commun.* **2010**, *46*, 8374–8376.
- [73] C. Reichardt, *Solvents and Solvents Effects in Organic Chemistry*, Wiley-VCH, Weinheim, **2003**, p. 433.
- [74] R. M. C. Gonçalves, A. M. N. Simoes, L. M. P. C. Albuquerque, M. Roses, C. Rafols, E. Bosch, *J. Chem. Res.* **1993**, 214–215.
- [75] L. Brooker, R. Sprague, C. Smyth, G. Lewis, *J. Am. Chem. Soc.* **1940**, *62*, 1116–1125.
- [76] P. Pasman, F. Rob, J. W. Verhoeven, *J. Am. Chem. Soc.* **1982**, *104*, 5127–5133.
- [77] S. Webster, J. Fu, L. A. Padilha, O. V. Przhonska, D. J. Hagan, E. W. Van Stryland, M. V. Bondar, Y. L. Slominsky, A. D. Kachkovski, *Chem. Phys.* **2008**, *348*, 143–151.
- [78] W. Liptay, *Angew. Chem.* **1969**, *81*, 195–206; *Angew. Chem. Int. Ed. Engl.* **1969**, *8*, 177–188.
- [79] W. Liptay, In *Excited States* (Ed.: E. Lim), Academic Press, New York, **1974**, p. 129.
- [80] A. Painelli, F. Terenziani, *J. Phys. Chem. A* **2000**, *104*, 11041–11048.
- [81] A. Painelli, F. Terenziani, D. Comoretto, *J. Phys. Chem. A* **2000**, *104*, 11049–11054.
- [82] A. Painelli, F. Terenziani, *Chem. Phys. Lett.* **1999**, *312*, 211–220.

Received: June 18, 2012

Revised: September 25, 2012

Published online: November 23, 2012